THE JOURNAL OF PHYSICAL CHEMISTRY LETTERS
A JOURNAL OF THE AMERICAN CHEMICAL SOCIETY

pubs.acs.org/JPCL

Letter

Understanding the Optimal Cooperativity of Human Glucokinase: Kinetic Resonance in Nonequilibrium Conformational Fluctuations

Weihua Mu,* Jing Kong, and Jianshu Cao*

Cite This: *J. Phys. Chem. Lett.* 2021, 12, 2900−2904

Read Online

ACCESS | Metrics & More | Article Recommendations | Supporting Information

ABSTRACT: The cooperativity of a monomeric enzyme arises from dynamic correlation instead of spatial correlation and is a consequence of nonequilibrium conformation fluctuations. We investigate the conformation-modulated kinetics of human glucokinase, a monomeric enzyme with important physiological functions, using a five-state kinetic model. We derive the non-Michealis−Menten (MM) correction term of the activity (i.e., turnover rate), predict its relationship to cooperativity, and reveal the violation of conformational detailed balance. Most importantly, we reproduce and explain the observed resonance effect in human glucokinase (i.e., maximal cooperativity when the conformational fluctuation rate is comparable to the catalytic rate). With the realistic parameters, our theoretical results are in quantitative agreement with the reported measurement by Miller and co-workers. The analysis can be extended to a general chemical network beyond the five-state model, suggesting the generality of kinetic cooperativity and resonance.

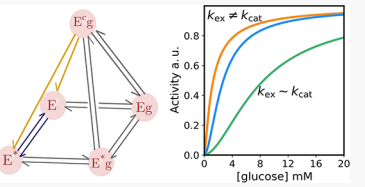

Single-molecule measurements have revealed the ubiquitous presence of conformational fluctuations in biomolecules.[1,2] In enzymes, these fluctuations lead to temporal correlations in single-molecule turnover sequences (i.e., memory effects) and possible deviations from the Michalies−Menten (MM) rate expression.[1,3−19] The MM kinetics are characterized by a hyperbolic dependence of the turnover rate on the substrate concentration [S], traditionally explained as a consequence of the steady-state solution on the ensemble level,[20,21] and have recently been extended to the conformational nonequilibrium steady state to account for slow conformational dynamics at the single-molecule level.[1,10,12] The conformational-modulated non-MM enzyme kinetics have been characterized by kinetic cooperativity[3−5,22] and have inspired intensive interest in theoretical studies.[10,12,19] In particular, using a novel integrated probability flux balance method, we explicitly derived the generalized MM expressions, established the relationship between the non-MM kinetics and nonzero conformational population current (i.e., broken conformational detailed balance), and constructed a phase diagram of the various types of cooperativity of monomeric enzymes.[12,23]

For allosteric enzymes with multiple binding sites, binding the substrate in one site enhances or inhibits the binding in the other site, leading to the positive (or negative) cooperativity.[22] The allosteric effect involves the correlation between two or more spatially separated binding states.[24,25] However, for a monomeric enzyme with a single binding site, the observed cooperativity results from the "temporal correlation" due to the nonequilibrium conformational dynamics instead of the spatial correlation. Detailed theoretical analysis has predicted positive or negative cooperativity as well as inhibition,[6,26] which were considered to be signatures of allosteric enzymes but can also result from conformational regulation in monomeric enzymes (the allokairic effect).[27,28] A recent experiment in human glucokinase (GCK) by Miller and co-workers has clearly demonstrated this possibility and motivates our theoretical calculation.[29] A monomeric enzyme with only one binding site, the structure of human GCK rules out the allosteric mechanism, implying the possibility of kinetic cooperativity.[30] It has been suggested that the cooperativity of human GCK that arises from the temporal transmission of the binding information, instead of the spatial transmission, resulting in the "allokairic" cooperativity or "dual allosteric activation mechanism".[29] The cooperativity of the human GCK is reported to be strongly modulated by the disease-induced mutations, implying that the activation mechanism of dual allosteric activation is relevant to the human's physiological functions. The mutation studies further suggest that the structure of human GCK is optimized by the selection from a variety of species with natural mutations. Therefore, understanding the working mechanism of human GCK has significant theoretical and biological implications.[31]

Reaction Network of Human GCK. With the structural information on the human GCK, a reaction network as shown in Figure 1(a) is proposed to describe the kinetic behavior of human GCK in the physiological range of the glucose concentration.[29] The five-state model is characterized by two distinct conformational states of an unliganded GCK,[32] which

Received: February 7, 2021
Accepted: March 11, 2021

https://doi.org/10.1021/acs.jpclett.1c00438
J. Phys. Chem. Lett. 2021, 12, 2900−2904

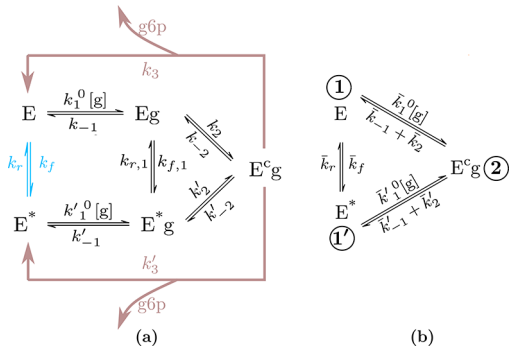

Figure 1. Reaction network of a human GCK: (a) The five-state model proposed by Miller and co-workers with the measured rate constants, $k_{cat} = k_3 + k'_3$, and (b) the effective three-state model reduced from the five-state model in (a), with $\bar{k}_2 = k_3$ and $\bar{k}'_2 = k'_3$. In this minimal model of the turnover cycle, both reactions associated with $\bar{k}_2$ and $\bar{k}_{-1}$ turn E^{c}g into E.

have higher and lower affinities for the glucose substrate. These two unliganded states, E and E*, interconvert with each other via the reversible reaction $E \underset{k_r}{\overset{k_f}{\rightleftharpoons}} E^*$ with the exchange rate constant $k_{ex} \equiv k_f + k_r$. In one turnover cycle, the two parallel conformational pathways start with two unliganded human GCK states, coupled by conformational transitions $E \underset{k_i}{\overset{k_f}{\rightleftharpoons}} E^*$ and $Eg \underset{k'_r}{\overset{k'_f}{\rightleftharpoons}} E^*g$. Then the two pathways converge to state E^{c}g, followed by a series of reactions described as an effective catalytic step, $E^cg \xrightarrow{k_3/k'_3} E/E^*+product$, and finally recover the unliganded state of human GCK. In fact, the human GCK's reaction produces both glucose 6-phosphate (g6p) and ADP. Since experimental evidence indicates the ordered binding of substrates (glucose first, followed by ATP) and the ordered release of products (ADP first, followed by g6p), the rate-limiting step is dominated by the glucose/g6p pair, so we do not consider the contribution of ATP/ADP in this work. There are more general scenarios beyond this simple case.

NMR measurements of the human GCK's enzymatic reaction demonstrate that the cooperativity is most prominent when the exchange rate constant k_{ex} is comparable to the catalytic constant, k_{cat}.[29] Here, k_{cat} represents the apparent catalytic rate constant of GCK to yield the product of glucose, corresponding to an effective one-step reaction composed of several consecutive steps. This observed resonance condition (i.e., $k_{ex} \approx k_{cat}$) suggests a possible way to inhibit the cooperativity of human GCK by altering the k_{ex} and/or k_{cat} to break the resonance of these two rate constants. The goal of our analysis is to solve the five-state model and rigorously establish the resonance condition of $k_{cat} \approx k_{ex}$.

To theoretically investigate the kinetic cooperativity of human GCK, it is necessary to study the nonequilibrium conformational dynamics of this five-state model shown in Figure 1(a). In general, the kinetics of a monomeric enzyme can be described by master equations, which dictate the time evolution of the probabilities of finding the enzyme at the various states (in the present case, these are P_E, P_{E^*}, P_{Eg}, P_{E^*g}, and P_{E^cg}). The master equation is supplemented by the probability conservation condition for one human GCK at different states during the turnover cycle, $\sum_{i=1}^{5} P_i = 1$ (where i denotes all five listed states of GCK). In the step $g + E \underset{k_{-1}}{\overset{k_1^0}{\rightleftharpoons}} Eg$, the concentration of glucose [g] is absorbed into the forward rate constant k_1^0, leading to a quasi-first-order forward reaction and a first-order reverse reaction $E \underset{k_{-1}}{\overset{k_1^0[g]}{\rightleftharpoons}} Eg$. Under the steady-state condition, the time deviation of P_i vanishes, leading to $P_{E^cg,ss}$ at steady state and the enzyme's activity $v = k_{cat}P_{E^cg,ss}$.

To simplify the analysis, we map this five-state model to an effective three-state model with only three GCK states (E, E*, and E^{c}g), denoted as 1, 1′, and 2, respectively. This three-state model is the minimal model for describing a turnover process of an enzyme with conformational fluctuations. In this effective model shown in Figure 1(b), the states are connected by the reactions with effective rate constants, which are chosen to reproduce the steady-state probabilities of E, E*, and E^{c}g as in the five-state model, $g + E \underset{\bar{k}_{-1}}{\overset{\bar{k}_1^0}{\rightleftharpoons}} E^cg$, $g + E^* \underset{\bar{k}_{-1}}{\overset{\bar{k}_1'^0}{\rightleftharpoons}} E^cg$, $E \underset{\bar{k}_r}{\overset{\bar{k}_f}{\rightleftharpoons}} E^*$, $E^cg \xrightarrow{\bar{k}_2} E + g6p$, and $E^cg \xrightarrow{\bar{k}'_2} E^* + g6p$, as also shown in Figure 1(b). Here the six rate constants in the effective three-state model are labeled as $\bar{k}_i$ to distinguish them from those in the original five-state model. Under steady-state conditions, the relationship between these two sets of rate constants is found to be $\bar{k}_2^{(\prime)} = k_3^{(\prime)}$, $\bar{k}_{f(r)} = k_{f(r)}$, $\bar{k}_1^{(\prime)0} = k_1^{(\prime)0}\gamma_1^{(\prime)}$, and $\bar{k}_{-1}^{(\prime)} = k_{-1}^{(\prime)}\gamma_2^{(\prime)}$. Here, $\gamma_1^{(\prime)} = 1 - k_{-1}^{(\prime)}k_c^{(\prime)}/\Delta$, $\gamma_2 = (k_{-2}k_c - k'_{-2}k_{r,1})/\Delta$, $\gamma'_2 = (k'_{-2}k'_c - k_{-2}k_{f,1})/\Delta$, $\Delta \equiv k_ck'_c - k_{r,1}k_{f,1}$, and $k_c^{(\prime)} \equiv k_{-1}^{(\prime)} + k_2^{(\prime)} + k_{f,1}^{(\prime)}$. The details of the derivation are shown in the Supporting Information. This mapping method can be applied to the model with more intermediate states beyond Eg and E*g, for example, a series of states labeled as E_1g, E_2g,..., E_Ng, E_1^*g,..., and E_N^*g,[23] as in Figure 3.

Effective Three-State Model and the Activity of Human GCK. It is convenient to use the effective three-state model for turnover cycles of human GCK, which reproduces the same expression of activity of GCK as that obtained from the original five-state model. The last steps after the formation of E^{c}g are combined into an effective reaction, $E^cg \xrightarrow{k_2/k'_2} E/E^* + g6p$, and the effective catalytic rate constant $k_{cat} \equiv \bar{k}_2 + \bar{k}'_2$.

$$\frac{dP_1}{dt} = -(\bar{k}_1^0[g] + \bar{k}_f)P_1 + \bar{k}_rP_{1'} + (\bar{k}_{-1} + \bar{k}_2)P_2$$

$$\frac{dP_2}{dt} = \bar{k}_1^0[g]P_1 + \bar{k}_1'^0[g]P_{1'} - (\bar{k}_{-1} + \bar{k}'_{-1} + \bar{k}_2 + \bar{k}'_2)P_2 \quad (1)$$

The conservation of the probability predicts the steady-state activity of human GCK as

$$\frac{1}{v} = \frac{1}{k_{cat}}\left(1 + \frac{A}{[g]} + \frac{B - A}{[g] + C}\right) \quad (2)$$

with

$$A = \frac{(\bar{k}_f + \bar{k}_r)(\bar{k}_{-1} + \bar{k}'_{-1} + \bar{k}_2 + \bar{k}'_2)}{\bar{k}_f\bar{k}_1'^0 + \bar{k}_r\bar{k}_1^0}$$

$$B = \frac{\bar{k}_1'^0(\bar{k}_{-1} + \bar{k}_2) + \bar{k}_1^0(\bar{k}'_{-1} + \bar{k}'_2)}{\bar{k}_1'^0\bar{k}_1^0}$$

$$C = \frac{\bar{k}_1'^0\bar{k}_f + \bar{k}_1^0\bar{k}_r}{\bar{k}_1'^0\bar{k}_1^0} \quad (3)$$

https://doi.org/10.1021/acs.jpclett.1c00438
J. Phys. Chem. Lett. 2021, 12, 2900−2904

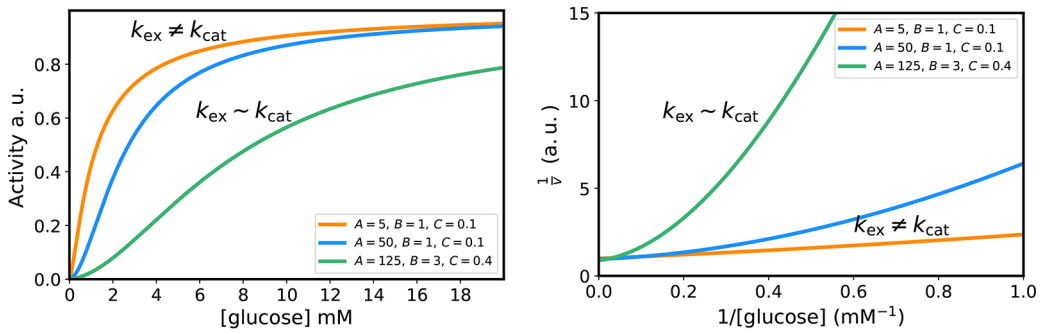

Figure 2. Substrate concentration dependence of the turnover rate (i.e., activity) of human GCK, calculated from the five-state model shown in Figure 1(a). (a) $v - [g]$ plots and (b) Lineweaver–Burk plots: $1/v - 1/[g]$. The Linewearver–Burk plots clearly show the cooperativity enhancement when the rate constants are $k_{ex} \approx k_{cat}$ (green line, $A = 125$, $B = 3$, and $C = 0.4$).

In terms of the rate constants in the original five-state model, coefficients A, B, and C become

$$A = \frac{(k_f + k_r)(k_{cat} + k_{-1}\gamma_{-1} + k'_1\gamma'_{-1})}{k_f k_1'^0\gamma'_1 + k_r k_1^0\gamma_1}$$

$$B = \frac{\zeta_1}{\zeta_2},\ C = \frac{k_f k_1'^0\gamma'_1 + k_r k_1^0\gamma_1}{\zeta_2}$$

Here, the two constants are given by

$$\zeta_1 \equiv (\delta_f + \delta_r)(k_{-1}\gamma_{-1} + k'_{-1}\gamma'_{-1} + k_{cat}) + k_1^0\gamma_1(k'_{-1}\gamma'_{-1} + k'_3) + k_1'^0\gamma'_1(k_{-1}\gamma_{-1} + k_3)$$

$$\zeta_2 \equiv (\delta_f + k_1^0\gamma_1)(\delta_r + k_1'^0\gamma'_1)$$

with $\delta_f \equiv k_1^0 k'_{-1}k_{f,1}/\Delta_A$, $\delta_r \equiv k_1'^0 k_{-1}k_{r,1}/\Delta_A$, and $\Delta_A = k_c k'_c - k_{r,1}k_{f,1}$. Equations 2 and 3 are the key formulas for investigating the cooperative kinetics of human GCK, which explains the observed correlation between the turnouver activity v and the ratio of rate constants $\{k_{ex}, k_{cat}\}$. The reduction of large networks to small ones greatly facilitates kinetic analysis. For this purpose, a self-consistent pathway approach not only provides a mapping procedure on the steady-state level[33] but also reduces an arbitrarily complex network to an irreducible scheme based on the waiting time distribution function formalism, which contains all of the statistical information beyond the steady-state solution.[26] The pathway analysis generalizes the MM equation, which has been analyzed in ref 26, and can also be applied to the network is this paper.

Kinetic Cooperativity. Obviously, truncated to the first two terms on the right-hand side of eq 2, the turnover rate reduces to the MM kinetics, $v = k_{cat}[g]/([g] + A)$. As is known, the cooperativity of an enzyme is described by the non-MM correction in the expression of activity v, which is the term that is proportional to $1/([g] + C)$ in eq 2. In ref 23, a parameter $\alpha \equiv B_1/B_0$ (or $\alpha = B/A - 1$ in terms of the present parameters) is introduced for the phase diagram. This parameter is a unique non-MM indicator for single-loop enzyme kinetics: (i) $\alpha \in [-1, 0)$ for the positive cooperativity, (ii) $\alpha > 0$ for the negative cooperativity, and (iii) $\alpha < 1$ for the substrate inhibition. Since positive cooperativity in the GCK kinetics was observed, we focus on the regime $0 < B \leq A$, where the larger the value of A, the closer α is to -1 and therefore the more positive the cooperativity.

Enzyme cooperativity is often described by the Hill equation in the form of[22]

$$\frac{1}{v} = \frac{1}{v_{max}}\left(1 + \frac{K_{0.5,glucose}^{n_H}}{[g]^{n_H}}\right) \quad (4)$$

The exponent n_H for the substrate concentrate $[g]$ is the Hill coefficient, which was reported to be $n_H \approx 1.6$ for the wild type of human GCK.[29,34] However, in the present expression of activity v given in eq 2, only the terms for the integer power of $[g]$ in the series expansion of $1/v$ are present. In general, we can use a power series to approximate a power-law function. Specifically, a truncated series $c_1/[g] + c_2/[g]^2$, with $c_1 = B$ and $c_2 = C(A - B) > 0$, is used to approach a power-law term $\sim 1/[g]^n$, with $1 < n < 2$ here.

Furthermore, the effective three-state kinetics can be reduced from the rectanglar four-state kinetics in refs 12, 23, and 35. As demonstrated in the previous studies, the cooperativity characterized by the parameter $\alpha \equiv B/A - 1$ results from the breakdown of the detailed balance.[23] This conclusion is still valid for the present effective three-state model of the single-loop system since the cooperativity vanishes at $\alpha = -1$ or $A = B$ if and only if

$$\bar{k}_1^0(\bar{k}_{-1} + \bar{k}_2)\bar{k}_f = \bar{k}_1'^0(\bar{k}'_{-1} + \bar{k}'_2)\bar{k}_r \quad (5)$$

The latter equation is exactly the detailed balance condition for the present three-state model. Thus, the three-state model can be considered to be a special case for the single-loop network discussed in refs 12, 23, and 35, with two nodes in a rectangular diagram that degenerate to one node. Using rate constants reported in the recent experiments,[29] three coefficients (A, B, and C) presented in eq 3 are all positive, implying that the cooperativity is most distinct when the value of A reaches its maximum. Typically, the value of the catalytic rate constant, k_{cat}, is much larger than those of the inverse reactions of the binding of the glucose to human GCK, $\bar{k}_{cat} \gg \bar{k}_{-1}\gamma_2 + \bar{k}'_{-1}\gamma'_2$, so that $A \propto (k_f + k_r)k_{cat}$. According to the arithmetic-geometric average inequality, $\sqrt{ab} \leq (a + b)/2$, $a, b > 0$, the product ab reaches its maximum if the summation $a + b$ is constant. Assuming $k_f + k_r + k_{cat}$ is roughly a constant in the range of $\sim(ms)^{-1}$, A reaches its maximum if and only if $k_{cat} \approx k_f + k_r \equiv k_{ex}$, which defines the resonance condition for the largest enhancement of the cooperativity, as shown in Figure 2(a,b). In particular, for the parameter set of $A = 125$, $B = 3$, and $C = 0.4$, Figure 2(a)

https://doi.org/10.1021/acs.jpclett.1c00438
J. Phys. Chem. Lett. 2021, 12, 2900−2904

perfectly reproduces the key features of experiments,[29,34] with Hill coefficient $n_H = 1.6$ and $K_{0.5\ glucose} \approx 8.8$ mM.

General Network. A general reaction network of human GCK-like enzymes with more conformation or intermedidate states can be studied in a similar procedure. In a typical network with $2N - 1$ states, as shown in Figure 3, p_{ij} ($i = 1, 2, j = 1, 2,..., N - 1$) and p_N denote the probabilities of this enzyme in the state labeled by the subscript. This model is a renewal process $p_N \rightarrow p_{11}(p_{21})$ and thus is distinct from the general model in refs 12 and 35. The activity of human GCK (turnover rate) is $v = k_{cat}p_N$. Here, for convenience, the substrate concentrate is denoted as $s = [S]$. Under the steady-state condition, the activity (turnover rate) v is given as $1/v = 1/(k_{cat}p_N) \propto 1/p_N$, where the p_N takes the general form $1/p_N = c_1 + (1/s^{2N-3})\mathcal{P}(s)/Q(s)$, $N \geq 3$. Here, $\mathcal{P}(s)$ and $Q(s)$ are both polynomials of s, with their degrees satisfying $\deg(\mathcal{P}) < \deg(Q) \leq 2N - 3$. This fraction can be decomposed to a summation of fractions by the usual fraction apart method,[36] giving

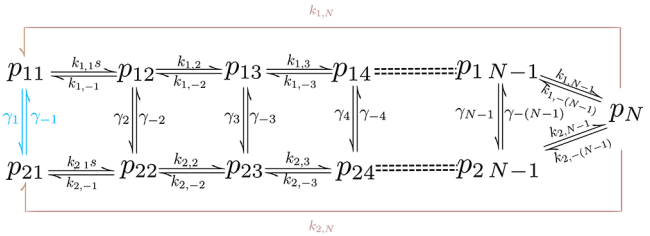

Figure 3. Schematic illustration of the general $2N - 1$ state model for the turnover of a monomeric enzyme. Each node denotes one conformational state in the reaction network, which is connected by a series of forward and backward reactions. Here, p_{ij} and p_N denote the probabilities that enzyme GCK stays in the corresponding states.

$$\frac{1}{v} = a_0 + \frac{b_0}{s} + \sum_{l=2}^{\bar{M}_0} \frac{b_l}{s^l} + \sum_{i=1}^{p} \sum_{m_i=1}^{\bar{M}_i} \frac{b_{i,m_i}}{(s + c_i)^{m_i}} + \sum_{j=1}^{q} \sum_{n_i=1}^{\bar{M}_j} \frac{\xi_{j,n_j} s + \zeta_{j,n_j}}{\left(s^2 + \phi_j s + \psi_j\right)^{n_j}},\ c_i \neq 0,\ \phi_j^2 < 4\psi_j \quad (6)$$

Here, $\{c_i\}$, $\{\phi_j\}$, and $\{\psi_j\}$ are real variables, $\{m_i\}$ and $\{n_j\}$ are positive integers, and $\phi_j^2 < 4\psi_j$ ensures that $(s^2 + \phi_j s + \psi_j)$ are the irreducible quadratic factors of $Q(s)$. In the denominator of the fraction shown in eq 6, the multiplicity of $(s^2 + \phi_j s + \psi_j)$ is $\bar{M}_j$. The multiplicity of a pole $-c_i$ of the polynomial $Q(s)$ is denoted as $\bar{M}_i$. This result is consistent with those in ref 35.

It is straightforward to verify that this general form of the activity of a monomeric enzyme recovers the classical MM kinetics if truncated at the leading two terms on the right-hand side of eq 6, leading to a hyperbolic curve of $v - [S]$.[20,21] Thus, all of the remaining terms in eq 6 contribute to the cooperativity of a monomeric enzyme characterized by the sigmoidal $v([S])$ curve. The activity described by eq 6 is a generalization of classical MM kinetics for the human GCK-type enzyme, as it clearly predicts the functional form of cooperativity in term of a series of fractions of $[S]$.

It is worth noting that, in the pioneering work of Neet and co-workers, the transients and cooperativity of enzyme kinetics were investigated using several kinetic models with slow conformational changes (denoted as "isomerization").[3] Interestingly, they also provided the functional expressions of the reciprocal of activity as a function of the reciprocal of the concentrate of the substrate and discussed the conditions for cooperativity as a result of the combination of rate constants. These early results bear a similarity to theoretical studies of enzyme cooperativity observed in single-molecule experiments, including our present work. Instead of transient dynamics, the present work focuses on the enhanced cooperativity (resonance) observed experimentally under the nonequilibrium steady-state condition. In this work and earlier publications, we have obtained the functional form of substrate dependence for arbitrarily complex networks of monomeric enzymes and thus established the relationship between kinetic cooperativity and the breakdown of the conformational detailed balance.

The key idea of our work is the nonequilibrium transitions between multiple conformation states. This type of conformational transition is related to the flexibility and stability of the protein in response to thermal fluctuations or external driving, which can potentially regulate enzyme activity. This topic is of broad interest and will be further explored in future studies.

In summary, we study the kinetic cooperativity of a human GCK, which exhibits enhanced cooperativity under conformation modulation, and establishes the resonance condition $k_{ex} \approx k_{cat}$. That is, the exchange rate constant for conformational fluctuations between two unliganded states of human GCK, k_{ex}, is comparable to the catalytic rate, k_{cat}. Using the five-state model proposed by the experimentalists with the measured parameters, we derive the turnover rate by considering the nonequilibrium conformational fluctuations. The functional expression of activity of a human GCK explicitly predicts a non-MM kinetic correction term, which results from violations of the conformational detailed balance, in consistent with the previous analysis of a general enzyme network with nonequilibrium conformations. Comparing this correction term with the Hill equation for enzyme cooperativity, we confirm the Hill coefficient to be 1 to 2 as reported experimentally and discuss the relationship between the non-MM correction and the kinetic cooperativity of a human GCK. Our theoretical calculations using the reported parameters are in quantitative agreement with recent experiments. This agreement verifies our prediction of the kinetic resonance of human GCK and reaffirms the validity of the general functional form of the enzyme's kinetics regulated by conformational dynamics. Our results for the kinetic cooperativity of human GCK can be extended to more complex networks, for example, allosteric enzymes with both temporal and spatial correlations in the turnover process.

■ ASSOCIATED CONTENT

Supporting Information

The Supporting Information is available free of charge at https://pubs.acs.org/doi/10.1021/acs.jpclett.1c00438.

Correspondence of the rate constants for the five- and three-state models of a human glucokinase; solution of the three-state model; and solution of the $2N - 1$-state general model (PDF)

■ AUTHOR INFORMATION

Corresponding Authors

Weihua Mu − *Wenzhou Institute, University of Chinese Academy of Sciences, Wenzhou 325001, China; Department of Electrical Engineering and Computer Science,*

https://doi.org/10.1021/acs.jpclett.1c00438
J. Phys. Chem. Lett. 2021, 12, 2900−2904

Massachusetts Institute of Technology, Cambridge 02139, U.K.; orcid.org/0000-0002-0338-7023; Email: muwh@wiucas.ac.cn

Jianshu Cao − *Department of Chemistry, Massachusetts Institute of Technology, Cambridge 02139, U.K.;* orcid.org/0000-0001-7616-7809; Email: jianshu@mit.edu

Author

Jing Kong − *Department of Electrical Engineering and Computer Science, Massachusetts Institute of Technology, Cambridge 02139, U.K.;* orcid.org/0000-0003-0551-1208

Complete contact information is available at: https://pubs.acs.org/10.1021/acs.jpclett.1c00438

Notes

The authors declare no competing financial interest.

■ ACKNOWLEDGMENTS

J.C. acknowledges NSF support (grant nos. CHE 1800301 and CHE 1836913). W.M. thanks Dr. Weiming Xu for helpful discussions of laboratory methods in enzymology.

■ REFERENCES

(1) English, B. P.; Min, W.; van Oijen, A. M.; Lee, K. T.; Luo, G.; Sun, H.; Cherayil, B. J.; Kou, S. C.; Xie, X. S. Ever-Fluctuating Single Enzyme Molecules: Michaelis-Menten Equation Revisited. *Nat. Chem. Biol.* **2006**, *2*, 87−94.
(2) Lu, H. P. Sizing up Single-Molecule Enzymatic Conformational Dynamics. *Chem. Soc. Rev.* **2014**, *43*, 1118−1143.
(3) Ainslie, G. R., Jr.; Shill, J. P.; Neet, K. E. Transients and Cooperativity. *J. Biol. Chem.* **1972**, *247*, 7088−7096.
(4) Frieden, C. Slow Transitions and Hysteretic Behavior in Enzymes. *Annu. Rev. Biochem.* **1979**, *48*, 471−489.
(5) Cornish-Bowden, A.; Cárdenas, M. L. Co-operativity in Monomeric Enzymes. *J. Theor. Biol.* **1987**, *124*, 1−23.
(6) Cao, J. Event-Averaged Measurements of Single-Molecule Kinetics. *Chem. Phys. Lett.* **2000**, *327*, 38−44.
(7) Gopich, I. V.; Szabo, A. Statistics of Transitions in Single Molecule Kinetics. *J. Chem. Phys.* **2003**, *118*, 454−455.
(8) Xue, X.; Liu, F.; Ou-Yang, Z.-c. Single Molecule Michaelis-Menten Equation beyond Quasistatic Disorder. *Phys. Rev. E* **2006**, *74*, 030902.
(9) Cao, J.; Silbey, R. J. Generic Schemes for Single-Molecule Kinetics. 1: Self-Consistent Pathway Solutions for Renewal Processes. *J. Phys. Chem. B* **2008**, *112*, 12867−12880.
(10) Min, W.; Xie, X. S.; Bagchi, B. Two-Dimensional Reaction Free Energy Surfaces of Catalytic Reaction: Effects of Protein Conformational Dynamics on Enzyme Catalysis. *J. Phys. Chem. B* **2008**, *112*, 454−466.
(11) Qian, H. Cooperativity and Specificity in Enzyme Kinetics: A Single-Molecule Time-Based Perspective. *Biophys. J.* **2008**, *95*, 10−17.
(12) Cao, J. Michaelis-Menten Equation and Detailed Balance in Enzymatic Networks. *J. Phys. Chem. B* **2011**, *115*, 5493−5498.
(13) Kolomeisky, A. B. Michaelis−Menten Relations for Complex Enzymatic Networks. *J. Chem. Phys.* **2011**, *134*, 155101.
(14) Ochoa, M. A.; Zhou, X.; Chen, P.; Loring, R. F. Interpreting Single Turnover Catalysis Measurements with Constrained Mean Dwell Times. *J. Chem. Phys.* **2011**, *135*, 174509.
(15) Piwonski, H. M.; Goomanovsky, M.; Bensimon, D.; Horovitz, A.; Haran, G. Allosteric Inhibition of Individual Enzyme Molecules Trapped in Lipid Vesicles. *Proc. Natl. Acad. Sci. U. S. A.* **2012**, *109*, E1437−E1443.
(16) Chaudhury, S.; Cao, J.; Sinitsyn, N. A. Universality of Poisson Indicator and Fano Factor of Transport Event Statistics in Ion Channels and Enzyme Kinetics. *J. Phys. Chem. B* **2013**, *117*, 503−509.
(17) Moffitt, J. R.; Bustamante, C. Extracting Signal from Noise: Kinetic Mechanisms from a Michaelis-Menten-like Expression for Enzymatic Fluctuations. *FEBS J.* **2014**, *281*, 498−517.
(18) Barato, A. C.; Seifert, U. Universal Bound on the Fano Factor in Enzyme Kinetics. *J. Phys. Chem. B* **2015**, *119*, 6555−6561.
(19) Barel, I.; Brown, F. L. H. On the Generality of Michaelian Kinetics. *J. Chem. Phys.* **2017**, *146*, 014101.
(20) Michaelis, L.; Menten, M. L. Die Kinetik der Invertinwirkung. *Biochem. Z.* **1913**, *49*, 333−369.
(21) Johnson, K. A.; Goody, R. S. The Original Michaelis Constant: Translation of the 1913 Michaelis-Menten Paper. *Biochemistry* **2011**, *50*, 8264−8269.
(22) Cornish-Bowden, A. *Fundamentals of Enzyme Kinetics*, 4th ed.; Wiley-Blackwell: Weinheim, Germany, 2012.
(23) Piephoff, D. E.; Wu, J.; Cao, J. Conformational Nonequilibrium Enzyme Kinetics: Generalized Michaelis−Menten Equation. *J. Phys. Chem. Lett.* **2017**, *8*, 3619−3623.
(24) Changeux, J. P. Allostery and the Monod-Wyman-Changeux Model after 50 Years. *Annu. Rev. Biophys.* **2012**, *41*, 103−133.
(25) Guo, Q.; He, Y.; Lu, H. P. Interrogating the Activities of Conformational Deformed Enzyme by Single-Molecule Fluorescence-Magnetic Tweezers Microscopy. *Proc. Natl. Acad. Sci. U. S. A.* **2015**, *112*, 13904−13909.
(26) Avila, T. R.; Piephoff, D. E.; Cao, J. Generic Schemes for Single-Molecule Kinetics. 2: Information Content of the Poisson Indicator. *J. Phys. Chem. B* **2017**, *121*, 7750−7760.
(27) Hilser, V. J.; Anderson, J. A.; Motlagh, H. N. Allostery vs. Allokairy. *Proc. Natl. Acad. Sci. U. S. A.* **2015**, *112*, 11430−11431.
(28) Porter, C. M.; Miller, B. G. Cooperativity in Monomeric Enzymes with Single Ligand-Binding Sites. *Bioorg. Chem.* **2012**, *43*, 44−50.
(29) Whittington, A. C.; Larion, M.; Bowler, J. M.; Ramsey, K. M.; Brüschweiler, R.; Miller, B. G. Dual Allosteric Activation Mechanisms in Monomeric Human Glucokinase. *Proc. Natl. Acad. Sci. U. S. A.* **2015**, *112*, 11553−11558.
(30) Cornish-Bowden, A. Understanding Allosteric and Cooperative Interactions in Enzymes. *FEBS J.* **2014**, *281*, 621−632.
(31) Thomas, D. D.; Corkey, B. E.; Istfan, N. W.; Apovian, C. M. Hyperinsulinemia: An Early Indicator of Metabolic Dysfunction. *J. Endocr. Soc.* **2019**, *3*, 1727−1747.
(32) Kamata, K.; Mitsuya, M.; Nishimura, T.; Eiki, J.; Nagata, Y. Structural Basis for Allosteric Regulation of the Monomeric Allosteric Enzyme Human Glucokinase. *Structure* **2004**, *12*, 429−438.
(33) Ninio, J. Alternative to the Steady-State Method: Derivation of Reaction Rates from First-Passage Times and Pathway Probabilities. *Proc. Natl. Acad. Sci. U. S. A.* **1987**, *84*, 663−667.
(34) Larion, M.; et al. Kinetic Cooperativity in Human Pancreatic Glucokinase Originates from Millisecond Dynamics of the Small Domain. *Angew. Chem., Int. Ed.* **2015**, *54*, 8129−8132.
(35) Wu, J.; Cao, J. In *Single-Molecular Biophysics: Experiment and Theory*; Komatsuzaki, T., Kawakami, M., Takahashi, S., Yang, H., Silbey, R. J., Eds.; Advances in Chemical Physics; John Wiley & Sons, Inc.: Hoboken, NJ, 2011; Vol. *146*, pp 329−365.
(36) Artin, M. *Algebra*, 2nd ed.; Pearson Education: Boston, 2010.